of JMA seismic intensity 7 or greater obtained through damage survey of the wooden houses in the Hyogo Prefecture after the 17 January 1995 Hyogo-ken Nambu earthquake comparing with the contours of depths to the base layers having the standard penetration resistance N of more than 50(Igarashi *et al.*,1995). It is interesting to note that most of heavily damaged areas were underlain by uneven surface base layers which outline the basin shapes. For this reason, our study aims at giving a simple and practical formulation which can evaluate site response affected by topographical irregularity especially focusing on uneven surface base layers. Lateral seismic design forces at the surface of the soft soil sedimentary layers underlain by the uneven surface base layers are defined in the form of the acceleration response spectra, finally.

SITE RESPONSE ANALYSES

In order to examine the fundamental site response characteristics affected by uneven surface base layers, two dimensional site response FEM analyses were conducted concerning two typical topographical models such as the inclined base(S type) and the basin(D type) as shown in Fig. 2. The dimension of irregular structures and the soil properties on Table 1. were changed parametrically. The inclination angle θ is changed for three cases in the inclined base model, i.e., tan θ =1/1,1/2 and 1/4. In the basin model, the width of central horizontal part B is changed for three cases, i.e., B=0, 40 and 80m. Here, the impedance ratio IP is $\rho_1 Vs_1 / \rho_2 Vs_2$. ρ is the mass density, Vs is the shear wave velocity and 1 and 2 refer to the surface layer and underlying base layer, respectively. H is the largest thickness of the surface layer having the constant value of 20m. Both the surface layer and base layer were assumed to be 5% damped elastic layers.

Fig. 3 shows the characteristics of input motion produced by fitting TAFT EW wave(1952) to the design acceleration response spectrum on the base layer outcroppings proposed by Design Code for Bridges in Japan(1990). Computer programs FLUSH by Lysmer *et al.*(1975) and FEM2D by Ishikawa *et al.*(1990) were employed for inplane and antiplane analyses, respectively. The viscous and energy transmitting boundaries were attached to the bottom and the both side ends within the base layers, respectively, assuming the vertical incident waves.

Fig. 4 shows the site amplification factors defined as the horizontal response spectral ratio of surface motions relative to base layer outcropping motions calculated for S2 and D1 models with all IP values. From both figures, it is known that Amax, the maximum amplification factor, is nearly proportional to IP values and TA*, the period having Amax, mainly depends on Vs1. Fig. 5 shows the distribution of Amax and TA* along the surface for all models with IP=1/6. The peak Amax arises on the soil profile changing area or near the end of deepest surface soil layer. Amax grows in proportion to θ in the inclined base models. TA* is dependent on the depths to the base layer. In the basin models, however, Amax takes the peak value at the center of the basin where the thickness of surface soil layer is largest and the distribution of Amax becomes gentle as the width of basin is wider. TA* is approximately constant along the surface and the larger the dimension of irregular structures is, the longer it becomes. These results were reflected to the formulation described in the next section.

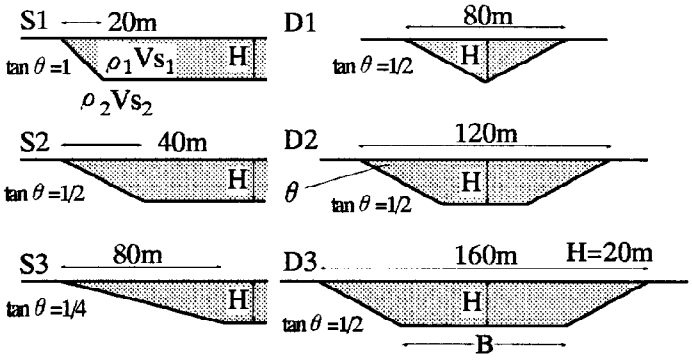

Fig. 2. Topographical models for response analyses

Table 1. Soil properties

Impedance ratio	$I_P=\frac{\rho_1 Vs_1}{\rho_2 Vs_2}$	1/6	1/4	1/3	1/2
Mass density	ρ_1,ρ_2(tf/m³)	1.8/9.8			
Surface layer S velocity	Vs_1(m/s)	100	150	200	150
Base layer S velocity	Vs_2(m/s)	600	600	600	300
Damping ratio	h_1,h_2	0.05			

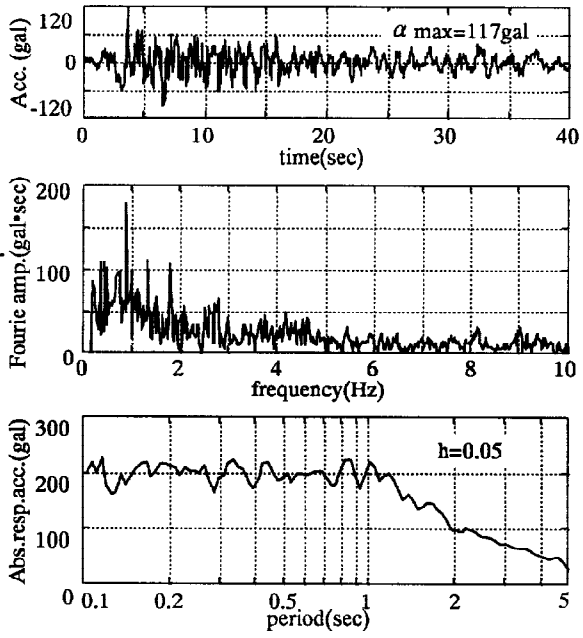

Fig. 3. The characteristics of input motion

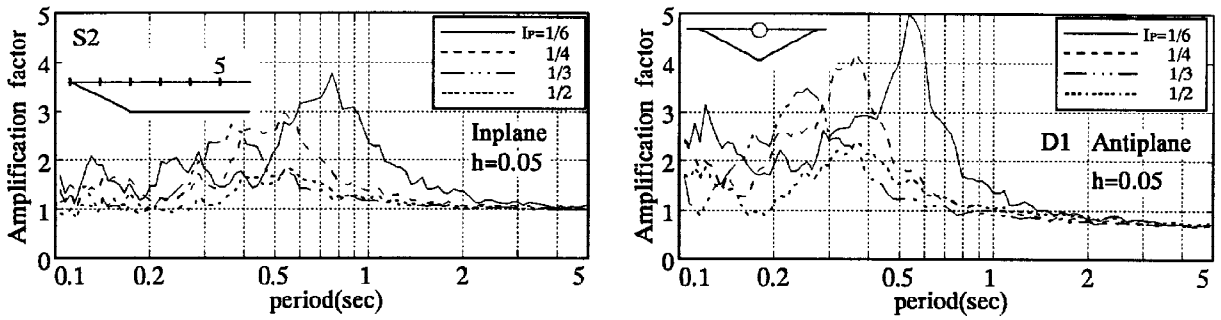

(a) S2 for each IP (b) D1 for each IP

Fig. 4. Spectral amplification factors between surface motion and base layer outcropping motion

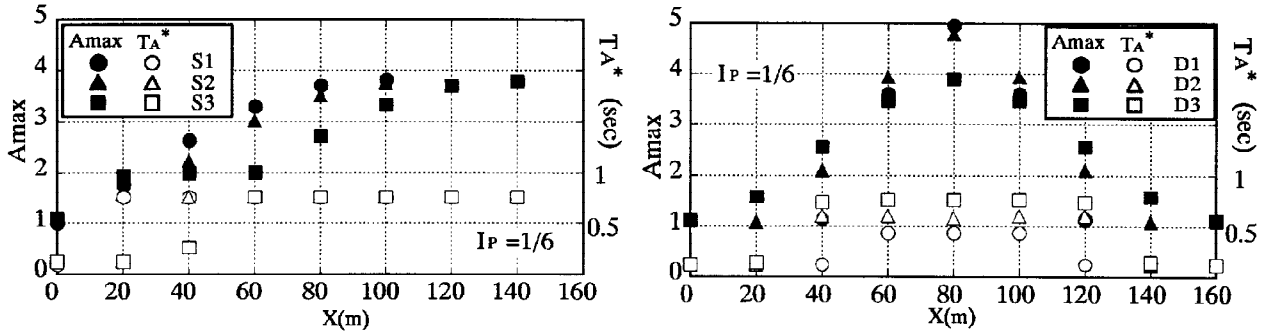

(a) S type for IP=1/6 (b) D type for IP=1/6

Fig. 5. Distribution of Amax and TA* related to the site location on the surface

FORMULATION

Definition of Design Spectra

Design horizontal acceleration response spectrum SA(T) at the surface of the soft soil sedimentary layers is defined as follows.

$$S_A(T)=C_S(T)*S_{Ab}(T) \tag{1}$$

SAb(T) is a standard horizontal response spectrum on the base layer outcroppings. T is a natural period of structure. Cs(T) represents the horizontal spectral amplification factor including the effects of uneven surface base layers. It is defined as the response spectral ratio of surface motions relative to base layer outcropping motions in the form like a response function of single-degree-of-freedom-system as follows.

$$C_S(T) = \frac{1}{\sqrt{\left(1-\frac{T_A^{*2}}{T^2}\right)^2 + \left(\frac{T_A^*}{T}\right)^2 / A_{max}^2}} \tag{2}$$

where, TA* is the fundamental period of surface soil layers including the topographical effects where the maximum amplification occurs. Amax is the maximum amplification factor due to the topographical effects and the wave-soils resonance effects depending on the impedance ratio and a function of the site location on the surface relative to the topographical irregular structure. In addition, Amax is assumed to be the following equation.

$$A_{max} = \sqrt{A_{Hmax}^2 + A_{imax}^2} \qquad (i = S, D) \tag{3}$$

AHmax is the maximum amplification factor due to the wave-soils resonance of vertically propagating waves in the surface layers. Aimax represents the maximum amplification factor due to the multiple reflections of horizontally propagating waves caused by the topographical irregular structures such as S type and D type.

Modeling of AHmax

1/IP is the theoretical undamped maximum amplification factor from two elastic horizontally layered model(surface layer and semi-infinite base layer) when the vertical incident wave is a harmonic wave with a period equal to the fundamental period(=4HX/VS1) of the elastic surface layer. Considering non-stationary random characteristics of earthquake ground motions and the damping of surface layers, the maximum amplification factor was empirically expressed as the square root of 2/IP. Consequently, AHmax is modeled by eq. (4). Where, β is a supplementary term concerning the thickness of surface layer. Hx is the depth to base layer and H0=20m is the standard depth.
Fig. 6 shows the comparison of AHmax from different methods. It can be seen that the AHmax estimated by eq. (4) has a good agreement with the values both from the response analysis using SHAKE by Schnabel *et al.*(1972) and Kanai's empirical formula(1966).

$$A_{Hmax} = \beta * \sqrt{\frac{2}{I_P}} \qquad (4)$$

where

$H_x \le 35m$

$$\beta = 0.8 \cdot \left\{\left[\frac{H_x}{H_0}\right]^2 + 0.25\right\} \cdot \exp\left\{1 - \left[\frac{H_x}{H_0}\right]\right\}$$

$H_0 = 20m$

$H_x \ge 35m \quad \beta = 1.25$

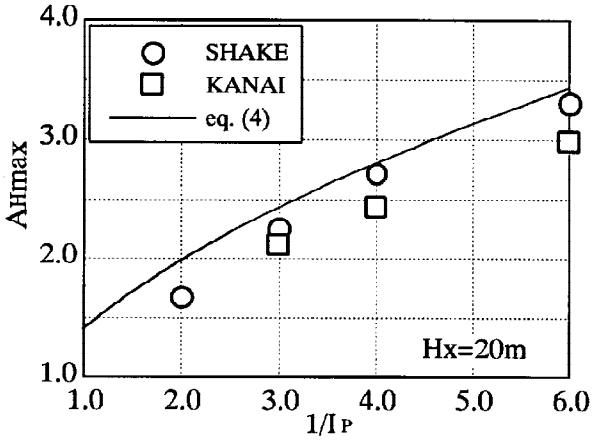

Fig. 6. Comparison of AHmax

Modeling of ASmax and ADmax

Derivation by the theory of elastic waves

Assume that horizontally propagating waves are generated on the left and right boundaries when the surface layer is shaken by a vertical incident wave with a amplitude A as shown in Fig. 7. Then, the generated four waves are expressed as follows.

$$\begin{aligned} U_{LO} &= B * \exp^{i\omega\left(t+\frac{x}{V_{S2}}\right)} \\ U_{LI} &= C * \exp^{i\omega\left(t-\frac{x}{V_{S1}}\right)} \exp^{-\eta x} \\ U_{RO} &= E * \exp^{i\omega\left(t-\frac{x'}{V_{S2}}\right)} \\ U_{RI} &= D * \exp^{i\omega\left(t+\frac{x'}{V_{S1}}\right)} \exp^{\eta x'} \end{aligned} \qquad (5)$$

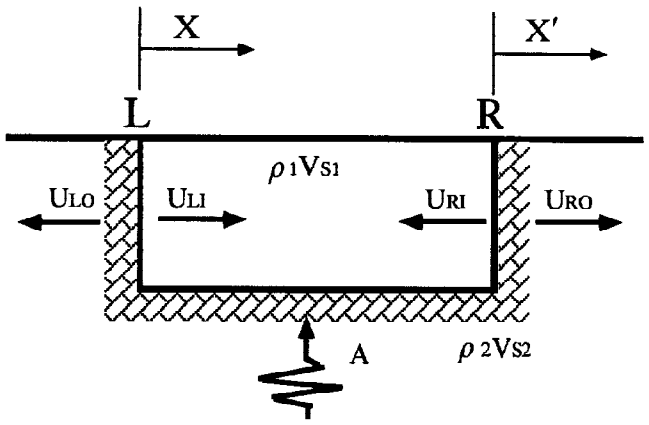

Fig. 7. Concept of horizontally propagating waves

where, i and ω represent the imaginary unit and the circular frequency, respectively. The exponential terms including the damping ratio η represents the effect of internal damping of surface layer. Generally, the damping of base layer is much smaller than that of surface layer and hence it is assumed to be negligible.
Let the continuities of displacements and forces be satisfied, the following equations are derived from eq. (5).

$$\begin{aligned} B &= C + D\Phi & \alpha_L B + CI_P - D\Phi I_P - f\alpha_L I_P &= 0 \\ E &= C\Phi + D & -C\Phi I_P + DI_P + \alpha_R E + f\alpha_R I_P &= 0 \end{aligned} \qquad (6)$$

where $I_P = \frac{\rho_1 V_{S1}}{\rho_2 V_{S2}} \qquad f = \frac{F}{\rho_1 V_{S1} i\omega} \qquad \Phi = \exp^{-L_W\left(\frac{i\omega}{V_{S1}}+\eta\right)}$

α_L and α_R are the wave blocking rates on each side boundary. Lw is width of the basin. F is the virtual force which acts on the both side boundaries and assumed to be as follows.

$$F = \kappa \frac{G_1}{V_{S1}} i\omega\left(\frac{1}{I_P} - 1\right)A \tag{7}$$

where, G1 is the shear modulus of surface layer soil, A is an amplitude of incident wave, κ is assumed to be 2. Consequently, the amplitudes of propagating and reflecting waves in the surface layer are solved as follows.

$$C = \frac{I_{Pf}\{(\alpha_R + I_P)\alpha_L + (\alpha_L - I_P)\alpha_R\Phi\}}{\{(\alpha_R + I_P)(\alpha_L + I_P) - (\alpha_R - I_P)(\alpha_L - I_P)\Phi^2\}} \tag{8}$$

$$D = \frac{-I_{Pf}\{(\alpha_L + I_P)\alpha_R + (\alpha_R - I_P)\alpha_L\Phi\}}{\{(\alpha_R + I_P)(\alpha_L + I_P) - (\alpha_R - I_P)(\alpha_L - I_P)\Phi^2\}} \tag{9}$$

In the case that side boundary exists only on one side, let $L_W \to \infty$, $\Phi \to 0$, $\alpha_L = \alpha_R = \alpha$, then the maximum amplification factor As becomes as follows.

$$A_S = \frac{|C|}{2A} = \frac{\alpha_L(1 - I_P)}{\alpha_L + I_P} = \frac{\alpha(1 - I_P)}{\alpha + I_P} \tag{10}$$

In the case that side boundaries exist on both sides, let $\eta \to 0$, exponential terms $\to 1$,then the maximum amplification factors A_{DL} and A_{DR} due to both-side boundaries become as follows.

$$A_{DL} = \frac{|C|}{2A} = \frac{(1 - I_P)\{I_P(\alpha_L - \alpha_R) + 2\alpha_L\alpha_R\}}{2I_P(\alpha_R + \alpha_L)} \tag{11}$$

$$A_{DR} = \frac{|D|}{2A} = \frac{(1 - I_P)\{I_P(\alpha_R - \alpha_L) + 2\alpha_L\alpha_R\}}{2I_P(\alpha_R + \alpha_L)} \tag{12}$$

Considering non-stationary random characteristics of earthquake ground motions and the damping of surface layers, the same operation for AHmax were performed for the maximum amplification factors derived here and they resulted in the formulation of ASmax and ADmax in the next section.

Formulation of ASmax, ADmax and T_A^*

Fig. 8 demonstrates two types of topographical model's schemata. Using some parameters shown in these figures, ASmax and ADmax, the maximum amplification factors, and T_A^*, the predominant period depending on the soil properties, soil profiles and the site location can be defined according to each topographical models as below.

Inclined base(S type)

$$T_A^* = \frac{4H_X}{V_{S1}} \tag{13}$$

$$A_{Smax} = \sqrt{\frac{2\alpha(1 - I_P)}{(\alpha + I_P)}} * \left(\frac{H_X - H_U}{H_L}\right) * \left(\frac{X}{L}\right) * \exp\left(1 - \frac{X}{L}\right) \tag{14}$$

Where, the wave blocking rate α denotes HL/H and the 3rd and 4th term in the right-hand side of eq. (14) express the empirical distribution function of the maximum amplification factors along X-axis on the surface. Hx is a depth to base layer at the location pointed by distance X. L represents the distance from side boundary where peak value of Asmax occurs as follows.

$$L = 4\sqrt{L_D * H_L} \tag{15}$$

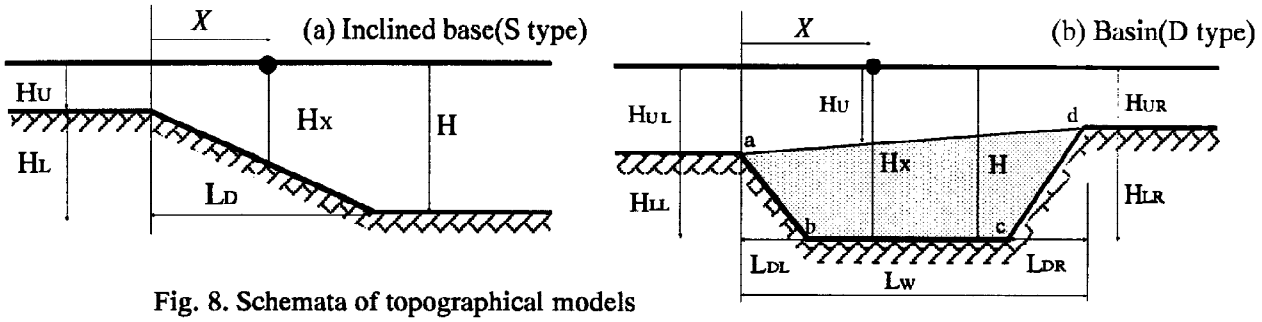

Fig. 8. Schemata of topographical models

Baisin(D type)

$$T_A^* = \frac{4H''}{V_{S1}} + \frac{4H_U}{V_{S1}} = \frac{4}{V_{S1}} * \frac{S}{L_W} + \frac{4H_U}{V_{S1}} \tag{16}$$

$$A_{Dmax} = \sqrt{\frac{(1-I_P)}{(\alpha_L+\alpha_R)I_P}} * \sqrt{A_{FL}^2 + A_{FR}^2} \tag{17}$$

Where, H'' is the equivalent depth given by the following equation.

$$H'' = \frac{S}{L_W} \tag{18}$$

S is the cross sectional area surrounded by a, b, c, and d shown in Fig. 8. The 1st term in the right-hand side of eq. (16) adopts the smaller value of 4H''/Vs1 or 4(Hx-Hu)/Vs1 when X is smaller than LDL or larger than Lw-LDR. In eq. (17), AFL and AFR express the amplification factors due to horizontally propagating waves generated on both side boundaries and they are combined in the form of the root mean square. The following equations represent them respectively.

$$A_{FL} = \sqrt{I_P(\alpha_L-\alpha_R)+2\alpha_L\alpha_R} * \left(\frac{H_X-H_U}{H_{LL}}\right) * \left(\frac{X}{L_L}\right) * \exp\left(1-\frac{X}{L_L}\right) \tag{19}$$

$$A_{FR} = \sqrt{I_P(\alpha_R-\alpha_L)+2\alpha_L\alpha_R} * \left(\frac{H_X-H_U}{H_{LR}}\right) * \left(\frac{L_W-X}{L_R}\right) * \exp\left(1-\frac{L_W-X}{L_R}\right) \tag{20}$$

Where, the wave blocking rates α_L and α_R denote HLL/H and HLR/H, respectively. LL and LR are given by

$$L_L = \sqrt{2 * L_{DL} * H_{LL}} \qquad L_R = \sqrt{2 * L_{DR} * H_{LR}} \tag{21}$$

VALIDATION

Comparison with the results from site response analyses and previous studies

Fig. 9 presents the distribution of Amax values on the surface evaluated by the constructed formulation comparing with those from the site response FEM analyses shown in previous section. It can be quickly seen from these figures that the Amax values evaluated by the formulation conform well with those from the analyses.
Fig. 10 shows the comparison between evaluated Amax values and those from previous studies by other researchers. From Fig. 10(a), (b) showing the comparison with BEM analyses (Seki *et al.*,1991) and seismic

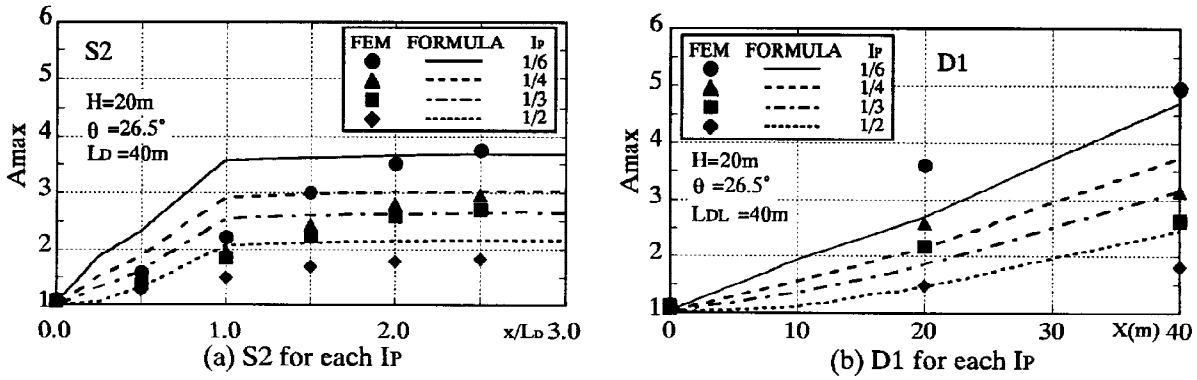

(a) S2 for each IP (b) D1 for each IP

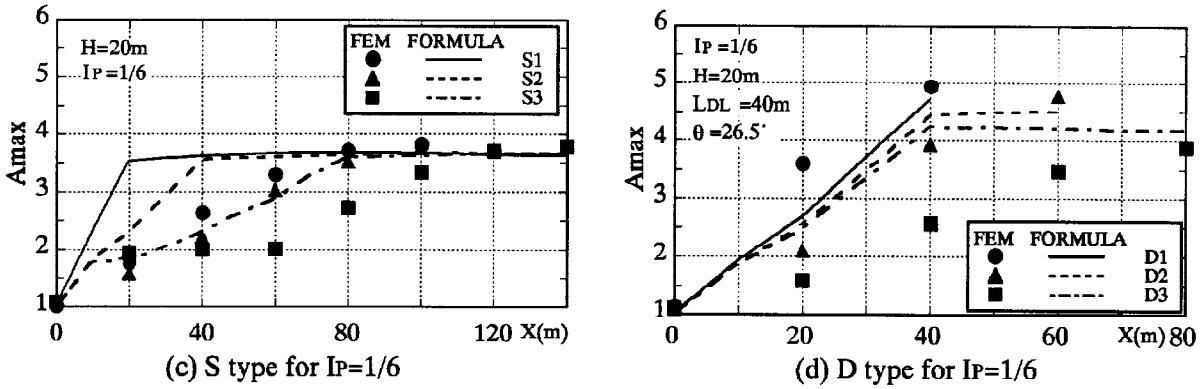

(c) S type for IP=1/6 (d) D type for IP=1/6

Fig. 9. Comparison of Amax between the formulation and the FEM analyses conducted here

observations (Ando *et al.*,1991), it is known that the formulation of S type structures can explain the distribution of the Amax values from previous studies. Fig. 10(c), (d) shows the comparison of Amax values on D type structures. The formulation of D type structures can explain the distribution of the Amax values from the FEM analyses (Tamura *et al.*,1989) shown in Fig. 10(c), but in Fig. 10(d) presenting the comparison with the microtremor observations (Imaoka *et al.*,1990), the Amax values evaluated by the formulation are smaller than those from the observations. It seems to be a reason for this difference that the Amax values from the microtremor observations are small strain parameters due to very weak motions.

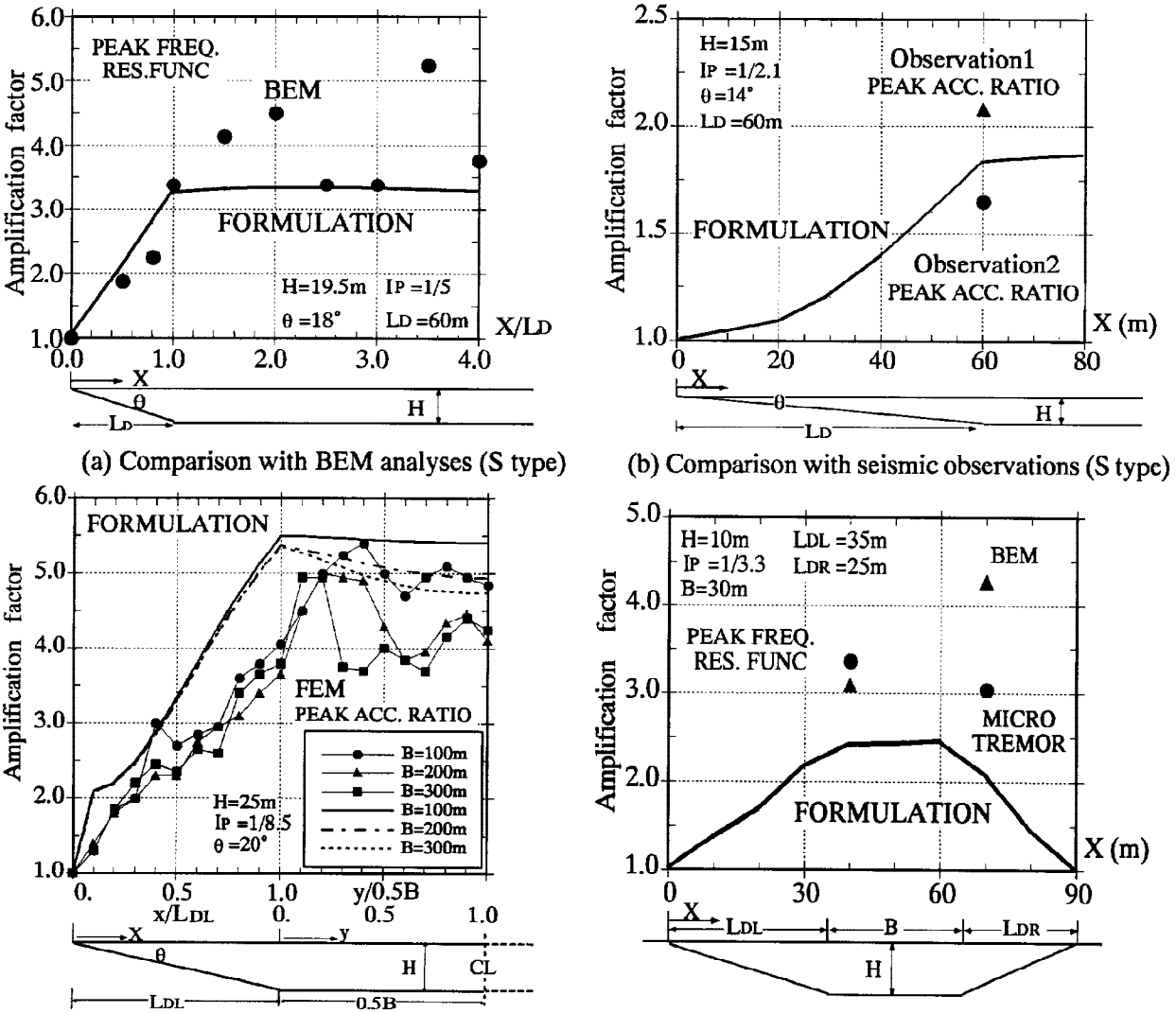

(a) Comparison with BEM analyses (S type) (b) Comparison with seismic observations (S type)

(c) Comparison with FEM analyses (D type) (d) Comparison with micro tremors (D type)

Fig. 10. Comparison of the amplification factors between the formulation and the previous studies

Extremest Amax by the formulation

Fig. 11 presents the comparison of the extremest Amax values among the different irregular structures calculated by eq. (4), (14) and (17), respectively. It is found that the Amax values from D type are about 1.5 times higher than AHmax values due to the flat layers on the average, whereas the values from S type exceed AHmax values by about 10 percent maximum.
So, it should be noted that the basin structures have a significant impact on the site specific response in comparison with other topographical irregular structures.

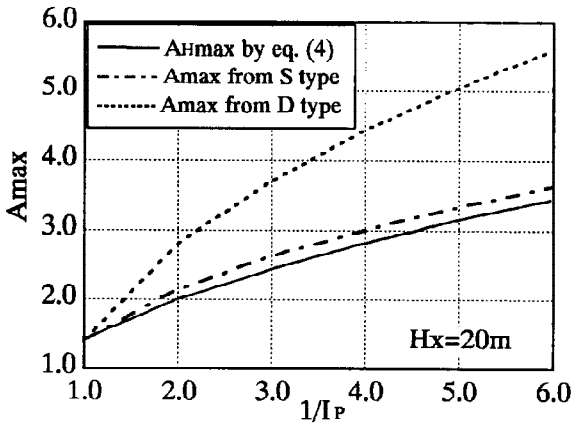

Fig. 11. Comparison of the extremest Amax among the different irregular structures

CONCLUSIONS

1) The site specific response affected by topographically uneven surface base layers can be expressed by a combination of two multiple reflections.
One consists of vertically propagating waves and the another consists of horizontally propagating waves.
2) The site amplification factors caused by the multiple reflections of horizontally propagating waves can be described by a set of simple formulas.
3) The maximum site amplification factor multiplying the acceleration response spectrum on the base layer outcroppings can be approximately related to the square root of the amplification factor due to a vertical incident harmonic wave with a period equal to the fundamental period of the elastic surface layer.
4) The site amplification factors evaluated by the formulation proposed here can explain those obtained from both the actual site response observations and the site response analyses.
5) This study depends on the theory of elastic waves. The non-linearity effects of the surface soil layers, however, can be easily taken into account by reflecting the results from the non-linear site response analyses using the equivalent linear technique.

REFERENCES

Ando, H. and Sase T.(1991) : The topographical effects on the buried pipelines seismic response, *JSCE No.21 Earthquake Engineering Symposium*, PP.49-52(in Japanese)

Ejiri, J. and Goto, Y.(1994) : Introduction of topographical effects on site response for design spectra, *Japan Soc.Civil.Eng.*, Report **No.501**, pp.173-182(in Japanese)

Igarashi, S., Moriguchi, H., Hisakawa, E., Suzuki, T. and Hakuno, M.(1995) : Relationship between vertical ground motion induced by topographic effects and structural damage, *JSCE No.23 Earthquake Engineering Symposium*, PP.77-80(in Japanese)

Imaoka, K. and Taga, N.(1990) : Dynamic behavior of structure and ground with irregular soil layer, *The eighth Japan Earthquake Engineering Symposium*, **Vol.2**, PP.415-419(in Japanese)

Ishikawa, R., Takano, S. and Yasui, Y.(1990) : Finite element method for obliquely incident seismic wave problems(Part2), *Technical Research Institute Report of Obayashi Corp.*, **No.41**, pp.20-25(in Japanese)

Japan Road Association(1990) : Design code for bridges -earthquake resistant design-, **Vol.V**(in Japanese)

Kanai, K., Tanaka, T., Yoshizawa, S., Morishita, T., Osada, K. and Suzuki, T.(1966) : Comparative studies of earthquake motions on the ground and underground II ,*Bulletin of ERI*, **Vol.44**, pp.609-643(in Japanese)

Kawase, H. and Aki, K.(1989) : A study on the response of a soft basin for incident S, P and Rayleigh waves with special reference to the long duration observed in Mexico City, *BSSA* , **Vol.79**, pp.1361-1382

Koketsu, K.(1991) : Seismic waves in irregularly layered media, Japan Soc.Civil.Eng.,Report No.437, pp.1-18

Lysmer, J., Udaka, T., Tsai, C.F. and Seed, H.B.(1975) : A computer program for approximate 3-D analysis of soil-structure interaction problems, *EERC*, Report **No.75-30**

Seki, T. and Nishikawa, T.(1991) : Surface ground motions on the irregular sediment-field supported elastic basin(Applied Sanchez-Sesma Method), *JSCE No.21 Earthquake Engineering Symposium*, PP.117-120 (in Japanese)

Seed, R.B., Dickenson, S.E. and Idriss, I.M.(1990) : Geotechnical factors controlling damage patterns in the Loma Prieta earthquake of October 17, 1989, *Special session of JGS No.25 annual conference*, PP.1-39

Schnabel, P.B., Lysmer, J. and Seed, H.B.(1972) : SHAKE-A computer program for earthquake response analysis of horizontally layered sites, *EERC*, Report **No.72-12**

Tamura, C. and Futokoro, T.(1989) : Fundamental study for the effects of the base irregularities on surface ground motions, *JSCE No.20 Earthquake Engineering Symposium*, PP.145-148(in Japanese)

Toki, K., Goto, Y., Ejiri, J. and Sawada, S.(1995) : A brief review of source effects and local site effects during Hyogo-ken Nanbu earthquake, *Journal of JSCE*, **Vol.80-9**, pp.32-43(in Japanese)

Tokida, K. ,Tamura, K. and Fukada, H.(1992) : Effects of geological irregularities on ground motion characteristics, *10WCEE*, pp.669-672